http://ansinet.com/itj

ITJ

ISSN 1812-5638

INFORMATION TECHNOLOGY JOURNAL

ANSInet
Asian Network for Scientific Information
308 Lasani Town, Sargodha Road, Faisalabad - Pakistan

Information Technology Journal 13 (1): 94-101, 2014
ISSN 1812-5638 / DOI: 10.3923/itj.2014.94.101

Sub-dictionary Based Sparse Representation for Efficient Super-resolution Image Reconstruction

[1]Hao-Xian Wang, [2]Zhe-Ming Lu, [1]Yong Zhang and [1]Zhuo-Zhi Diao
[1]School of Information and Electrical Engineering,
Harbin Institute of Technology, Weihai, 264209, China
[2]School of Aeronautics and Astronautics, Zhejiang University, Hangzhou, 310027, China

Abstract: Super-resolution image reconstruction is an important digital image processing technique, which can improve the visual effects of images or serve as a pre-processing technique. Because of its impressive reconstruction results, sparse representation based super-resolution image reconstruction has become the focus of recent research. In order to alleviate the high computational complexity of the traditional sparse representation schemes, this study presents a fast sub-dictionary-based super-resolution reconstruction method. For each small input image block, a sub-dictionary is adaptively selected and thus the high-dimensional redundant dictionary-based sparse representation vector is replaced by a low-dimensional sub-dictionary based representation vector, the computational complexity is therefore reduced. Experimental results demonstrate that the proposed method can enhance the visual effects of images with a significantly low computational complexity.

Key words: Super-resolution image reconstruction, sparse representation, redundant dictionary, sub-dictionary

INTRODUCTION

Image reconstruction and image identification are two important topics in image analysis (Rahiman *et al*., 2012; Chen *et al*., 2012; Salehi and Mahdavi-Nasab, 2012). For a number of imaging devices, their detector arrays do not own enough density to appropriately sample the scene according to the required field of view, Super Resolution (SR) image reconstruction aims to estimate a High Resolution (HR) image from a single or a set of Low Resolution (LR) observations, which can be used for displaying LR images obtained from LR imaging devices on HR devices, it is therefore widely applied to various areas such as medical image processing, satellite remote sensing, high definition television standards and city security systems. With the development of SR image reconstruction techniques in the past several years, there have been three main types of SR image reconstruction techniques at the moment, i.e., conventional multi-frame based reconstruction algorithms (Hardie *et al*., 1997; Farsiu *et al*., 2004; Protter *et al*., 2009), interpolation-based algorithms (Hou and Andrews, 1978; Carrato *et al*., 1996; Li and Orchard, 2001; Giachetti, 2010) and machine learning based algorithms (Freeman *et al*., 2002; Zhang *et al*., 2010; Yang *et al*., 2008).

Conventional multi-frame based SR image reconstruction algorithms make full use of multiple LR images captured from the same scene to generate a SR image. Three typical conventional methods that have widely been researched are Maximum a Posteriori (MAP) (Belekos *et al*., 2010), Projection onto a Convex set (POCS) (Ogawa and Haseyama, 2011) and Iterative Back Projection (IBP) (Song *et al*., 2010). They are based on the same model and they are designed to obtain the HR images by imposing different additional constraints on ill-posed problems. In order to take advantage of the information from multiple input LR images, it is necessary to perform sub-pixel motion vector estimation on the input image sequences. Thus, too many parameters such as motion vectors and the settings of fuzzy matrices for these conventional schemes are required to be estimated. However, the input information is insufficient, the reconstruction results are therefore unsatisfactory.

Interpolation-based algorithms are the most simple and real-time methods and they often serve as the preprocessing step for other SR image reconstruction schemes. Two typical ones are bilinear interpolation and bicubic interpolation. They do not consider the intrinsic structure such as edges in images, thus resulting in image blurring or false edges. To overcome these problems, an

Corresponding Author: Hao-Xian Wang, School of Information and Electrical Engineering,
Harbin Institute of Technology, Weihai, 264209, China

adaptive interpolation techniques (Carrato *et al*., 1996) spatially adapt the interpolation coefficients to better match the local structures around the edges. Another method based on edge-directed interpolation (Li and Orchard, 2001) computes the local covariance coefficients from an LR image and then the coefficients are adopted to guide the interpolation process. Here, the pixels from the same structure are assigned with large weights, while others with small ones.

Machine learning based algorithms first learn the prior information based on the LR images and their corresponding HR images in the database, the SR image reconstruction is then guided based on the prior information. Freeman *et al*. (2002) modeled the spatial relationships between LR patches and HR patches using a Markov network, estimated the missing high-frequency content due to degradation and added it to the initial interpolation result to obtain the output HR image. Baker and Kanade (2000) proposed to learn a prior on the spatial distribution of the image gradient for frontal images of faces, where three types of pyramids: Gaussian pyramid, Laplacian pyramid and feature pyramid are introduced to denote the image feature space, whose parent structure is gained from the HR training images and a MAP cost function with respect to the high-resolution is established to achieve the image enhancement. This algorithm can yield 4-8 fold improvements in resolution, but because it needs too many paired low-resolution and high-resolution image blocks, the process is quite complicated and time consuming.

In the past two decades, sparse representation has been extensively utilized in a number of inverse image processing problems including denoising (Elad and Aharon, 2006) and restoration (Mairal *et al*., 2008). Research reports in sparse signal representation have shown that the linear relationship among the high-resolution signals could be estimated from their low-dimensional projections (Candes, 2006; Donoho, 2006). It is impossible to reconstruct the original image precisely since the SR problem is an ill-posed problem. However, some experiments have demonstrated both effectiveness and robustness of the sparse representation in regularizing the inverse problem. Yang *et al*. (2008) suggested an algorithm to choose the most relevant neighbors for reconstruction utilizing sparse coding. In this method, there is an assumption that the sparse representation of the HR patch is the same as that of the corresponding LR one. Based on this assumption, they tried to estimate the HR patch from the input image for each LR patch. In their local model, there are two dictionaries, D_l and D_h. D_h is composed of HR patches and D_l is composed of corresponding LR patches. For each input LR patch y, a sparse representation with respect to D_l is first found and the corresponding HR patches D_h is then combined according to these coefficients to generate the output HR patch. The main drawback of this method is its large dictionaries with expensive computation, resulting from the strategy that the dictionaries are obtained by random sampling a large number of patches from training images. To overcome this drawback, (Yang *et al*., 2010) proposed a different simple strategy by learning a more compact dictionary pair with a large number of image patch pairs to release the computational burden. However, due to the high-dimensional redundant dictionary, the solution of high-dimensional sparse coefficients leads to high computational complexity relatively.

As a result of impressive results, sparse representation based SR image reconstruction has been the focus of recent research in the SR filed. To reduce the complexity in building dictionary pairs during the training phase, reference (Lu *et al*., 2012) adopts a regularized orthogonal matching pursuit algorithm to solve the unknown coefficients, at the same time, the training efficiency has been improved partly. In this study, compared with the aforementioned sparse representation based methods, a sub-dictionary instead of redundant dictionary with high dimension is adaptively selected for each patch, aiming to speed up the algorithm while maintaining its performance.

PROPOSED IMAGE RECONSTRUCTION ALGORITHM

According to the compressed sensing theory, a sparse signal can be successfully recovered from a small number of linear measurements (Donoho, 2006). Specifically, suppose there is a redundant dictionary pair $\{D_h, D_l\}$, where D_h is for HR patches and D_l is for LR patches. Let X and Y denote the HR and LR images, respectively and x and y denote the HR and LR image patches, respectively. Given a LR patch, the problem of finding the sparsest representation of y_i can be formulated as:

$$z_i = \arg\min_{z_i}\left\{\|D_l z_i - y_i\|_2^2 + \lambda|z_i|_1\right\} \quad (1)$$

where, λ is a balance parameter and z_i is the sparse representation coefficient of y_i. In Reference (Lee *et al*., 2007), an efficient sparse coefficient solution method called feature-sign search algorithm is introduced. By solving Eq. 1 individually for each local patch, the HR patch can be reconstructed as:

$$x_i = D_h z_i \quad (2)$$

where, $x_i \in R^{M\times 1}$. Collecting all the HR patches $\{x_i\}$ to their corresponding positions and performing normalization, an initial estimation of the HR image X_0 can be obtained. Since the reconstruction is operated on each patch, it will cause unexpected pseudo-edge between adjacent patches. In order to improve the quality of HR image, the global reconstruction constraint is enforced by adopting the iterative back projection algorithm:

$$X = \arg\min_X \left\{ \|BHX - Y\|_2^2 + \beta \|X - X_0\|_2^2 \right\} \quad (3)$$

Here, the matrix B denotes the downsampling operation, H denotes the blurring operation related to the imaging system Point Spread Function (PSF), β is the balance parameter and X is the final target HR image.

To assure that the sparse representation of the HR patch with respect to D_h approximates to the sparse representation of the corresponding LR patch with respect to D_l, the coupled dictionaries are learned according to the following optimization process:

$$\{D_h, D_l, Z\} = \arg\min_{D_h, D_l, Z} \left\{ \|X_c - D_c Z\|_2^2 + \lambda |Z|_1 \right\} \quad (4)$$

Where:

$$X_c = [\frac{1}{\sqrt{M}} X_H^T, \frac{1}{\sqrt{N}} Y_L^T]^T$$

$X_H = [x_1, x_2,...]$ is the vector concatenated with HR patches and $Y_H = [y_1, y_2,...]$ is the vector concatenated with LR patches:

$$D_c = [\frac{1}{\sqrt{M}} D_h^T, \frac{1}{\sqrt{N}} D_l^T]^T$$

is the coupled high-low resolution dictionary trained from X, M and N denote the dimensions of the HR patches and LR patches, respectively and $Z = [z_1, z_2,...]$ is the matrix whose columns are the sparse representation vectors. The solution to Eq. 4 can be efficiently computed using the following iterative method:

Step 1: Initialize D_c with a normalized random Gauss matrix

Step 2: Update Z by adopting the feature-sign search algorithm (Lee *et al*., 2007) with fixed D_c

Step 3: Update D_c by addressing a quadratic programming problem with fixed Z

Step 4: Repeat Step 2 and Step 3 until the convergence is reached to obtain the coupled redundant dictionaries

The above-mentioned sparse representation based SR image reconstruction scheme can generate HR images with state-of-the art results. However, the sparse representation based SR image reconstruction algorithm adopts Eq. 1 to perform the sparse decomposition and in order to generate perfect HR images, the required dimension s of the redundant dictionary $D_l \in R^{r\times s}$ is high. That is to say, the redundant dictionary contains a lot of sparse bases, which leads to the high computational complexity. Experimental results demonstrate that the computational complexity has some connection with the dimension s (Yang *et al*., 2010; Lee *et al*., 2007): The higher the dimension s is, the more the computational complexity is. In addition, the higher dimension s also results in the higher dimension of the sparse coefficient z_i, which makes the computational complexity much higher. In other words, reducing the complexity of sparse coefficient computation for each input patch can reduce the complexity of the SR image reconstruction algorithm. Reference (Deng and Cao, 2009) proposed a multi-atoms rapid matching pursuit algorithm for signal sparse decomposition, where the redundant dictionary is partitioned into several incoherent sub-dictionaries, at each iteration, at most one matching atom is selected from each sub-dictionary to form a multi-atoms set and the multi-atoms signal approximation is achieved by orthogonal projection on the space of multi-atoms. Lee *et al*. (2001) proves that it is effective to represent an image patch by a few image patches with similar patterns. In this study, instead of adopting image patches to form redundant dictionary, the sub-dictionaries are trained from patches with similar patterns.

Because each sub-dictionary is obtained by training image patches with similar patterns, any image patch with similar patterns can be approximated sparsely with respect to the corresponding sub-dictionary, which means a lower dimension s can be selected. In this study, suppose $D_L = \{D_{l1}, D_{l2},..., D_{lP}\}$ and $D_H = \{D_{h1}, D_{h2},..., D_{hP}\}$ are HR sub-dictionaries and corresponding LR sub-dictionaries respectively, P stands for the number of sub-dictionary and $M' = [m_1, m_2,.., m_P]$ denotes the index vectors of sub-dictionaries adaptively selected for every input signal. To adaptively select the appropriate sub-dictionary for every input signal, the input LR image patch y_i is compared with every sub-dictionary index vector individually and the sub-dictionary is selected based on the minimum distance:

$$k_i = \arg\min_k \|y_i - m_k\|_2 \quad k = 1, 2, \pm \cdots P \tag{5}$$

Then, a LR sub-dictionary D_{li} and its corresponding HR sub-dictionary are used to replace the pairs of redundant dictionaries in Eq. 1 and 2 to generate the initial target HR images.

Suppose $F = [X_H, Y_L]$ are the pairs of training patches obtained from the training image database, $X_H = [x_1, x_2,..., x_r]$ are the HR image p atches used to train LR sub-dictionaries, $Y_L = [y_1, y_2,...y_r]$ are the corresponding LR image patches used to train HR sub-dictionaries. To get the sub-dictionaries, the dataset $Y_L = [y_1, y_2,...y_r]$ is clustered into several clusters by adopting the K-means algorithm, then X_H can be divided into several clusters correspondingly according to the clusters of Y_L. After that, a cluster of HR image patches or LR image patches is trained to obtain the corresponding sub-dictionary.

Suppose $X_L = [x_{H1}, x_{H2},...x_{Hr}]$ and $Y_L = [y_{L1}, y_{L2},...y_{LP}]$ denote the clustering results, where P is the total number of clusters. The index vector of every cluster can be obtained by calculating the centroid of each cluster as:

$$m_i = \frac{1}{n}\sum y_k \quad y_k \in Y_{li} \tag{6}$$

The corresponding sub-dictionary can be obtained as:

$$\{D_{hi}, D_{li}, Z_i\} = \arg\min_{D_{hi}, D_{li}, Z_i} \left\{\|X_{ci} - D_{ci} Z_i\|_2^2 + \lambda |Z_i|_1\right\} \tag{7}$$

Where:

$$X_{ci} = [\frac{1}{\sqrt{M}} X_{hi}^T, \frac{1}{\sqrt{N}} X_{li}^T]^T$$

$$D_{ci} = [\frac{1}{\sqrt{M}} D_{hi}^T, \frac{1}{\sqrt{N}} D_{li}^T]^T$$

Applying the above procedures to all of the sub-datasets X_{hi} and Y_{li}, all the HR dictionaries $D_H = \{D_{h1}, D_{h2},\cdots D_{hP}\}$, all the corresponding LR dictionaries $D_L = \{D_{l1}, D_{l2},\cdots D_{lP}\}$ and index vectors $M' = [m_1, m_2,\cdots m_P]$ can be obtained.

EXPERIMENTAL RESULTS

In order to evaluate the effectiveness of the proposed algorithm, several images are selected to test the proposed algorithm. For color images, the proposed algorithm is applied to the luminance channel only, while the color channels (Cb, Cr) are interpolated by the bicubic interpolation to the desired size.

The first step for dictionary training is to obtain the training vectors called feature patches. Here, the procedure to obtain LR image feature patch is given as follows: Firstly, perform the downsampling operation on the input HR images in the image database to obtain the LR images. Secondly, perform the upsampling operation on the obtained LR images to get the images with the same size as the original HR images. Thirdly, perform the convolution operation on the images obtained from the second step using four high frequency extracting factors in Eq. 8 to obtain four high frequency images:

$$\begin{aligned} f_1 &= [-1, 0, 1]; & f_2 &= f_1^T \\ f_3 &= [1, 0, -2, 0, 1]; & f_4 &= f_3^T \end{aligned} \tag{8}$$

Finally, partition the four high frequency images into patches. In this study, the patch size is 5×5. Suppose y_i^1, y_i^2, y_i^3 and y_i^4 are the four vectors that denote the ith patches in the four high frequency images, they can be concatenated to obtain a feature vector $y_i = [y_i^1, y_i^2, y_i^3, y_i^4]^T$.

The ith HR patch x_i can be obtained as follows: Firstly, partition the original HR images into patches. Secondly, arrange each patch as a vector. Finally, subtract the mean value from each element of the vector to get x_i.

Given an input LR image, the LR image patch for reconstruction can be obtained following the same procedure as for dictionary training mentioned above to obtain the LR image feature patch. In the experiment, the magnification factor is set to 2. For the LR patches, to eliminate the block effect, there is an overlap of 1 pixel between adjacent patches. The number of training vectors is 100000, which is partitioned into 50 clusters, the size (the number of sparse bases) of the sub-dictionary is set to S = 96.

To objectively evaluate the reconstruction performance, several evaluating indicators including MSE (Mean Square Error), PSNR (Peak Signal to Noise Ratio) and SSIM (Structural Similarity Index) are adopted in this study. The MSE between the original and a reconstructed high-resolution image is defined as:

$$MSE = \frac{1}{MN}\sum_{i=1}^{M}\sum_{j=1}^{N}(f(i, j) - g(i, j))^2 \tag{9}$$

where, f (i, j) and g (i, j) denote the original and the reconstructed image respectively, MN is the number of pixels. The corresponding PSNR is defined as:

$$PSNR = 10\lg\frac{255^2}{MSE} \tag{10}$$

As a specific example Wang *et al.* (2004) develops a measure of structural similarity that compares local patterns of pixel intensities that have been normalized for luminance and contrast, the measure can combine objective and subjective measures tightly:

$$SSIM(f,g)=\frac{(2\mu_f\mu_g+C_1)(2\sigma_{fg}+C_2)}{(\mu_f^2+\mu_g^2+C_1)(\sigma_f^2+\sigma_g^2+C_2)} \quad (11)$$

Here, μ_f and μ_g, respectively denote the mean intensity of image f (i, j) and g (i, j) and their standard deviations are denoted as σ_f and σ_g, respectively. σ_{fg} is the correlation coefficient between f (i, j) and g (i, j), C_1 and C_2 are small constants.

Because the size of the dictionary is decreased by adopting the sub-dictionary for sparse representation, the constraint parameter λ of the second term in Eq. 1 should be adjusted correspondingly. In order to select the most appropriate value for λ, the traversing operation is performed on λ and several LR images are used to generate the HR images and then calculate the average PSNR using the reconstructed HR images. Figure 1 shows the average PSNR of 9 HR images under different λ taking values from 0.05-0.55. From this figure, the highest average PSNR value can be obtained when λ is 0.35.

For the sake of checking the reconstruction performance, the SR image reconstruction visual performance of the proposed method is compared with that of the bicubic interpolation algorithm and the original sparse representation based SR image reconstruction algorithm (Yang *et al.*, 2010). The results of these algorithms on several test images are shown in Fig. 2. The adopted magnification factor is 2. In Fig. 2, the first column shows the LR images, the second column shows the HR results using bicubic interpolation, the third column shows the HR results using the original sparse representation based method and the last column is the corresponding results using the proposed algorithm. From Fig. 2, it can be seen that the proposed method can generate similar results to the algorithm in Yang *et al.* (2010) and visually much better than conventional methods such as the bicubic interpolation algorithm.

To quantitatively compare the speed and accuracy between above-mentioned algorithms, the quantitative comparison results are summarized in Table 1 and 2. The MSE and SSIM values are summarized in Table 1, from which, it can be seen that the proposed method generates better results than the bicubic interpolation, while nearly the same result as the algorithm in Yang *et al.* (2010). In Table 2, the time consuming of the proposed method is compared with the algorithm in Yang *et al.* (2010), where the speed up factor is defined as:

$$\text{Speed up factor}=\frac{\text{Time consumed by Yang } et\ al.\ (2010)}{\text{Time consumed by the proposed}} \quad (12)$$

From Table 1-2, it can be seen that the proposed method can generate the SR reconstruction results with desirable quality in terms of MSE and SSIM while enjoys a significant improvement in computational efficiency compared to the algorithm in Yang *et al.* (2010).

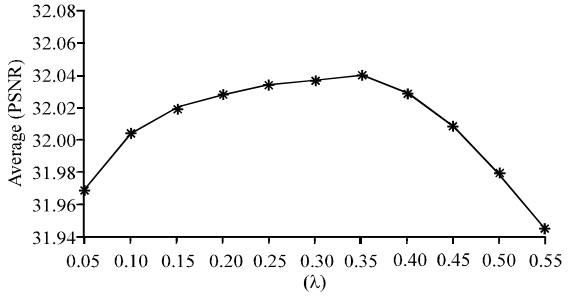

Fig. 1: Average PSNR of 9 HR images under different λ taking values from 0.05-0.55

Table 1: Comparison of estimation quality in SR image reconstruction (magnification factor: 2)

	MSE			SSIM		
Image	BICUBIC algorithm	Algorithm by Yang *et al.* (2010)	Proposed method	BICUBIC algorithm	Algorithm by Yang *et al.* (2010)	Proposed method
Lina	5.845	4.609	4.924	0.886	0.910	0.904
Butterfly	10.807	7.165	8.478	0.899	0.945	0.923
Girl	4.666	4.300	4.353	0.802	0.823	0.822
Parrots	6.883	5.252	5.683	0.925	0.941	0.936
Parthenon	10.012	8.755	9.078	0.788	0.835	0.826
Raccoon	7.241	6.065	6.308	0.841	0.889	0.884
Flower	7.658	5.961	6.374	0.882	0.922	0.913
Leaves	10.823	7.160	8.335	0.920	0.964	0.947
Hat	6.610	5.129	5.559	0.881	0.913	0.904

Fig. 2(a-d): SR image reconstruction results based on different methods, (a) Original LR images, (b) Results based on the bicubic interpolation algorithm, (c) Results using the original sparse representation based algorithm by Yang *et al*. (2010) and (d) Results based on the proposed algorithm

Table 2: Comparison of time complexity in SR image reconstruction (magnification factor: 2)

Image	Size	Time consuming of the algorithm by Yang *et al*. (2010) (sec)	Time consuming of the proposed algorithm (sec)	Speed up factor
Lena	256×256	74.989	12.205	6.144
Butterfly	256×256	71.445	11.244	6.354
Girl	256×258	74.621	12.093	6.170
Parrots	256×256	73.452	12.592	5.833
Parthenon	460×292	157.675	25.370	6.215
Raccoon	328×300	122.569	17.972	6.820
Flower	256×256	71.043	11.657	6.094
Leaves	256×256	67.311	11.046	6.094
Hat	256×256	74.137	11.307	6.557

CONCLUSION

An efficient sparse representation based SR image reconstruction method is proposed in this study. Because of the high dimension of sparse representation coefficients, the computational complexity of the original sparse representation based SR image reconstruction method is relative high. In this study, rather than using the redundant dictionary with high dimension, a sub-dictionary is adaptively selected to calculate the representation vector. Experimental results demonstrate that the proposed scheme can not only maintain the perfect visual effect, but also decrease the computational complexity.

ACKNOWLEDGMENT

This study is partially supported by the Zhejiang Provincial Natural Science Foundation of China under Grant R1110006 and Natural Scientific Research Innovation Foundation in Harbin Institute of Technology under Grant HIT. NSRIF. 2011115. The authors also gratefully acknowledge the helpful comments and suggestions of the reviewers, which have improved the presentation.

REFERENCES

Baker, S. and T. Kanade, 2000. Hallucinating faces. Proceedings of the 4th IEEE International Conference on Automatic Face and Gesture Recognition, March 28-30, 2000, Grenoble, France, pp: 83-88.

Belekos, S.P., N.P. Galatsanos and A.K. Katsaggelos, 2010. Maximum a posteriori video super-resolution using a new multichannel image prior. IEEE Trans. Image Process., 19: 1451-1464.

Candes, E.J., 2006. Compressive sampling. Proceedings of the International Congress of Mathetmaticians, Volume 3, August 22-30, 2006, Madrid, Spain, pp: 1433-1452.

Carrato, S., G. Ramponi and S. Marsi, 1996. A simple edge-sensitive image interpolation filter. Proceedings of the International Conference on Image Processing, September 16-19, 1996, Lausanne, pp: 711-714.

Chen, R.C., Y.K. Chan, Y.H. Chen and C.T. Bau, 2012. An automatic drug image identification system based on multiple image features and dynamic weights. Int. J. Innovat. Comput. Inform. Control., 8: 2995-3013.

Deng, C.Z. and H.Q. Cao, 2009. Multi-atoms rapid matching pursuit algorithm with incoherent sub-dictionary. Signal Process., 25: 613-617 (In Chinese).

Donoho, D.L., 2006. Compressed sensing. IEEE Trans. Inform. Theory, 52: 1289-1306.

Elad, M. and M. Aharon, 2006. Image denoising via sparse and redundant representations over learned dictionaries. IEEE Trans. Image Process., 15: 3736-3745.

Farsiu, S., M.D. Robinson, M. Elad and P. Milanfar, 2004. Fast and robust multiframe super resolution. IEEE Trans. Image Process., 13: 1327-1344.

Freeman, W.T., T.R. Jones and E.C. Pasztor, 2002. Example-based super-resolution. IEEE Comput. Graph. Appl., 22: 56-65.

Giachetti, A., 2010. Irradiance preserving image interpolation. Proceedings of the 20th International Conference on Pattern Recognition, August 23-26, 2010, Istanbul, pp: 2218-2221.

Hardie, R.C., K.J. Barnard and E.E. Armstrong, 1997. Joint map registration and high-resolution image estimation using a sequence of undersampled images. IEEE Trans. Image Process., 6: 1621-1633.

Hou, H.S. and H. Andrews, 1978. Cubic splines for image interpolation and digital filtering. IEEE Trans. Acoustics Speech Signal Process., 26: 508-517.

Lee, A., K. Pedersen and D. Mumford, 2001. The complex statistics of high-contrast patches in natural images. Proceedings of the IEEE Workshop on Statistical and Computational Theories of Vision, January 2001, France.

Lee, H., A. Battle, R. Raina and A.Y. Ng, 2007. Efficient sparse coding algorithms. Proceedings of Conference on Advances in Neural Information Processing Systems, December 4-7, 2006, Vancouver, British Columbia, Canada, pp: 801-808.

Li, X. and M.T. Orchard, 2001. New edge-directed interpolation. IEEE Trans. Image Process., 10: 1521-1527.

Lu, J., Q. Zhang, Z. Xu and Z. Peng, 2012. Image super-resolution reconstruction algorithm using over-complete sparse representation. Syst. Eng. Electron. Technol., 34: 403-408 (In Chinese).

Mairal, J., G. Sapiro and M. Elad, 2008. Learning multiscale sparse representations for image and video restoration. Multiscale Model. Simul., 7: 214-241.

Ogawa, T. and M. Haseyama, 2011. Missing intensity interpolation using a kernel PCA-based POCS algorithm and its applications. IEEE Trans. Image Process., 20: 417-432.

Protter, M., M. Elad, H. Takeda and P. Milanfar, 2009. Generalizing the nonlocal-means to super-resolution reconstruction. IEEE Trans. Image Process., 18: 36-51.

Rahiman, M.H.F., R.A. Rahim, H.A. Rahim, S.Z.M. Muji and E.J. Mohamad, 2012. Ultrasonic tomography-image reconstruction algorithms. Int. J. Innovative Comput. Inform. Control., 8: 527-538.

Salehi, S. and H. Mahdavi-Nasab, 2012. New image interpolation algorithms based on dual-tree complex wavelet transform and multilayer feedforward neural networks. Int. J. Innovat. Comput. Inform. Control., 8: 6885-6902.

Song, H., X. He, W. Chen and Y. Sun, 2010. An improved iterative back-projection algorithm for video super-resolution reconstruction. Proceedings of the Symposium on Photonics and Optoelectronic (SOPO), June 19-21, 2010, Chengdu, pp: 1-4.

Wang, Z., A.C. Bovik, H.R. Sheikh and E.P. Simoncelli, 2004. Image quality assessment: From error visibility to structural similarity. IEEE Trans. Image Process., 13: 600-612.

Yang, J., J. Wright, T. Huang and Y. Ma, 2008. Image super resolution as sparse representation of raw image patches. Proceedings of the IEEE Conference on Computer Vision and Pattern Recognition, June 23-28, 2008, Anchorage, AK., pp: 1-8.

Yang, J., J. Wright, T.S. Huang and Y. Ma, 2010. Image super-resolution via sparse representation. IEEE Trans. Image Process., 19: 2861-2873.

Zhang, K., X. Gao, X. Li and D. Tao, 2010. Partially supervised neighbor embedding for example-based image super-resolution. IEEE J. Selected Top. Signal Process., 5: 230-239.